Research Article

Laminin-coated multifilament entubulation, combined with Schwann cells and glial cell line-derived neurotrophic factor, promotes unidirectional axonal regeneration in a rat model of thoracic spinal cord hemisection

https://doi.org/10.4103/1673-5374.289436

Received: February 3, 2020

Peer review started: February 18, 2020

Accepted: May 8, 2020

Published online: August 10, 2020

Ling-Xiao Deng[1, 2], Nai-Kui Liu[1, 2], Ryan Ning Wen[3], Shuang-Ni Yang[1, 2], Xuejun Wen[4], Xiao-Ming Xu[1, 2, *]

Abstract

Biomaterial bridging provides physical substrates to guide axonal growth across the lesion. To achieve efficient directional guidance, combinatory strategies using permissive matrix, cells and trophic factors are necessary. In the present study, we evaluated permissive effect of poly (acrylonitrile-co-vinyl chloride) guidance channels filled by different densities of laminin-precoated unidirectional polypropylene filaments combined with Schwann cells, and glial cell line-derived neurotrophic factor for axonal regeneration through a T10 hemisected spinal cord gap in adult rats. We found that channels with filaments significantly reduced the lesion cavity, astrocytic gliosis, and inflammatory responses at the graft-host boundaries. The laminin coated low density filament provided the most favorable directional guidance for axonal regeneration which was enhanced by co-grafting of Schwann cells and glial cell line-derived neurotrophic factor. These results demonstrate that the combinatorial strategy of filament-filled guiding scaffold, adhesive molecular laminin, Schwann cells, and glial cell line-derived neurotrophic factor, provides optimal topographical cues in stimulating directional axonal regeneration following spinal cord injury. This study was approved by Indiana University Institutional Animal Care and Use Committees (IACUC #:11011) on October 29, 2015.

Key Words: axonal regeneration; extracellular molecule; filament density; hemisection; laminin; neurotrophic factor; Schwann cell; spinal cord injury; thoracic; transplantation

Chinese Library Classification No. R453; R741; R364.5

Introduction

The failure of axonal regeneration is the major barrier for functional recovery after spinal cord injury (SCI). Although combinatorial strategies to promote axonal regeneration have been applied to target complex pathophysiological processes (McKeon et al., 1995; Grimpe et al., 2002; Liu et al., 2006, 2007; Titsworth et al., 2008), agreement on success has not yet been obtained in understanding of the molecular-, cellular-, and systems-level support of axonal growth. One of the important reasons is the lack of animal model capable to rigorously distinguish regeneration from sprouting of spared axons. The most clinic relevant model is contusive SCI which however has difficulty in predicting the range of severed axon and distinguishing the regenerated axons. The transection model including either complete transection or incomplete transection (hemisection) utilizes a precise, clean approach by incision in specific target areas (Talac et al., 2004). Complete transection provides convincing evidences of axonal regeneration, however, lead to high mortality and severe injury hard for significant functional recovery. Unilateral hemisection injury like we used in this study can preserve the structural integrity and function of one side of the spinal cord sufficient to maintain bladder and bowel function. The regeneration of specific axonal pathways that project unilaterally in the spinal cord can be studied while their counterparts on the intact side serve as internal control. Hemisection can restore cerebrospinal fluid circulation after dura repair ensuring the delivery of nutrients to the graft tissue and prevent of connective tissue invasion to the graft region. This model also creates more stable cord-graft interfaces. Combined with guidance channel which provides a modifiable channel environment, there is great potential to test different trophic factors, matrix molecules and cell types in their ability to promote axonal regeneration.

For efficient axonal regeneration, it is essential to provide a physical substrate that allows axons to regenerate in unidirectional orientation. The common feature of successful regenerative approaches is the ability to either directly

[1]Spinal Cord and Brain Injury Research Group, Stark Neurosciences Research Institute, Indiana University School of Medicine, Indianapolis, IN, USA; [2]Department of Neurological Surgery, Indiana University School of Medicine, Indianapolis, IN, USA; [3]Maggie L. Walker Governor's School, Richmond, VA, USA; [4]Institute for Engineering and Medicine, Department of Chemical and Life Science Engineering, Virginia Commonwealth University, Richmond, VA, USA

*__Correspondence to:__ Xiao-Ming Xu, PhD, xu26@iupui.edu.

https://orcid.org/0000-0002-7229-0081 (Xiao-Ming Xu)

Funding: *Research in the Xu laboratory is supported by NIH 1R01 100531, 1R01 NS103481, Merit Review Award I01 BX002356, I01 BX003705, I01 RX002687 from the U.S. Department of Veterans Affairs, and Mari Hulman George Endowment Funds.*

How to cite this article: *Deng LX, Liu NK, Wen RN, Yang SN, Wen X, Xu XM (2021) Laminin-coated multifilament entubulation, combined with Schwann cells and glial cell line-derived neurotrophic factor, promotes unidirectional axonal regeneration in a rat model of thoracic spinal cord hemisection. Neural Regen Res 16(1):186-191.*

guide the axonal outgrowth along a unidirectional aligned topography or induce an aligned glial population to provide a cellular substrate to direct regenerating axons (Rangappa et al., 2000; Zhang et al., 2005; Sorensen et al., 2007). Polypropylene filaments have created an increasing pattern of alignment and outgrowth of dorsal root ganglion neurites in the direction parallel the long axis of the packed filament bundles of sub-cellular size (5 μm) *in vitro* (Wen and Tresco, 2006). However, whether these polymer filaments can promote the CNS neurite outgrowth is unknown.

In this study, we hypothesized that in a rodent model of hemisection spinal cord, transplantation of entubulation sleeves filled with different densities of 5 μm filaments combined with surface adhesive molecule laminin, glial cell line-derived neurotrophic factor (GDNF) and Schwann cells (SCs) would enhance directional growth of regenerated axons.

Materials and Methods

Device fabrication

Solutions of poly(acrylonitrile-co-vinyl chloride) (PAN-PVC) polymer in dimethysulphoxide (DMSO; Sigma-Aldrich, St. Louis, MO, USA) were prepared by mixing 12.5 wt% PAN-PVC and 87.5 wt% DMSO. Semipermeable, phase-inversion membranes were formed with a rough outer surface (outer diameter: 1000 μm) and a smooth inner surface (inner diameter: 900 μm). Isotactic polypropylene powder (average molecular weight = 250 kDa, Sigma-Aldrich) was thermally extruded at 170°C into filaments of 5 μm diameter. The diameters of the filaments were examined using transmission electron microscopy (Zeiss, Oberkochen, Germany). Filaments were reeled into longitudinally oriented bundles, inserted into PAN-PVC hollow fiber membranes. Filament bundles were coated with type 1 mouse laminin (10 μg/mL; Gibco, Rockville, MD, USA), Matrigel (BD Biosciences, San Jose, CA, USA) at 200 μg/mL in PBS, or thiol-functionalized hyaluronic acid (HA-SH)-based hydrogel (Biomaterials USA, Richmond, VA, USA) for 1 hour and rinsed with 0.1 M PBS for 2 hours in a 37°C incubator with 5% CO_2.

Experimental group assignment

A total of 88 adult female Sprague-Dawley rats (8 weeks of age, body weight 180–200 g, Harlan, Indianapolis, IN, USA) were randomly divided into the groups described below. In the first set of experiment (four groups, n = 8/group), we tested the effect of different filament density on axonal growth. PAN-PVC hollow channels packed with 1000, 2000, and 4000 filaments were defined as low, middle and high density groups and were compared with empty channels as controls. In the second set of experiment (four groups, n = 8/group), we examined the effects of different coating materials including laminin, Matrigel, and hydrogel by precoating them on low density channels since such density promoted the greatest axonal regeneration. No coating filaments served as control. In the last set of experiment (three groups, n = 8/group), we tested the efficacy of the combination of laminin-precoated low density filaments, SCs, and GDNF. Channels containing SCs/GDNF but no filament or channels containing laminin precoated filament but no SCs/GDNF were served as controls.

Spinal cord hemisection and transplantation of guidance channels

The procedures for spinal cord hemisection and mini-guidance channel implantation, as well as for pre- and post-operative animal care, were described in detail in previous publications (Xu et al., 1999; Bamber et al., 2001; Iannotti et al., 2003). Briefly, rats were anesthetized with sodium pentobarbital (45 mg/kg, i.p.; Abbott Laboratories, North Chicago, IL, USA). Following laminectomy at the 9th and 10th thoracic (T) vertebrae, the dura mater was incised longitudinally. A 2.5–2.8 mm gap lesion was created on the right side spinal cord. After removal of the hemi-cord, a mini-guidance channel of 3 mm-long was implanted into the gap. For channels containing SCs and GDNF, the final cells density was 120 × 10^6 cells/mL and final concentration of GDNF was 1 μg/μL. Rats were sacrificed at 4 weeks post-implantation. All animal handling, surgical procedures, and post-operative care were performed in accordance with the Guide for the Care and Use of Laboratory Animals and the Guidelines and Policies for Rodent Survival Surgery and approved by Indiana University Institutional Animal Care and Use Committees (IACUC #:11011) on October 29, 2015.

Light and transmission electron microscopy

At 4 weeks after transplantation, rats were transcardially perfused with 4% paraformaldehyde in 0.01 M phosphate buffered saline (PBS, pH 7.4). The spinal cord was then carefully dissected and a 1-mm transverse section was removed from the mid-point of the guidance channel and transferred to a fixative solution containing 2.5% glutaraldehyde and 5% sucrose in 0.1 M cacodylate buffer (pH 7.4) overnight. Transverse slices of the grafts taken at their midpoint were immersed in 1% osmium tetroxide in 0.1 M cacodylate buffer for 1 hour. Tissues were then dehydrated in graded ethanol and propylene oxide, and embedded in Spurr's epoxy resin. Transverse 1 μm-thick semi-thin plastic sections were stained in 1% toluidine blue-1% sodium borate (Sigma, St. Louis, MO, USA) to quantify the mean number of myelinated axons, blood vessels, and the mean tissue cable cross-sectional areas under an Olympus BX60 microscope equipped with a Neurolucida system (MicroBrightField, Colchester, VT, USA). For electron microscopy (EM) (Zeiss, Oberkochen, Germany), thin-sections were stained with uranyl acetate and lead citrate (Sigma, St. Louis, MO, USA) and examined using a Zeiss 108 transmission electron microscope (Zeiss, Oberkochen, Germany) at a magnification of 5000×.

Immunohistochemistry

The rostral and caudal segments of the grafted guidance channel, along with attached host cord segments were sectioned longitudinally on a cryostat (Leica CM3050, Nussloch, Germany) at 20–25 μm. The sections were rinsed in PBS, blocked, and permeabilized in PBS containing 10% normal goat serum and 0.3% Triton X-100 for 1 hour at room temperature, and incubated in primary antibodies overnight at 4˚C. Monoclonal antibody PhosphoDetect anti-neurofilament H mouse mAb (SMI-31) (1:1000; Chemicon, Temecula, CA, USA), mouse anti rat anti-CD68 (ED-1) (1:100; Millipore Antibodies, Billerica, MA, USA), mouse anti rat glial fibrillary acidic protein (GFAP) (1:300; Sigma-Aldrich), Nerve growth factor receptor (NGFR) P75 (1:200; Sigma-Aldrich) were used to identify axons, macrophages, astrocytes and SCs (Liu et al., 2004, 2007; Titsworth et al., 2007, 2008). On the following day, sections were incubated with either fluorescein-conjugated goat anti-rabbit (1:100, ICN Biochemicals, Aurora, OH, USA) or rhodamine-conjugated goat anti-mouse antibodies (1:100, ICN Biochemicals), and Hoechest 33342 (10 μg/mL, Sigma-Aldrich). Slides were examined with an Olympus BX60 microscope (Olympus America, Inc., Melville, NY, USA). Primary antibody omission and mouse and rabbit isotype controls (Zymed Lab Inc., San Francisco, CA, USA) were used to confirm the specificity of the antibodies.

Assessment of GFAP and ED1 *in vivo*

We used the GFAP staining as the astrogliosis reaction marker and ED1 staining as inflammatory marker. We measured the fluorescence intensity of GFAP and ED-1 immunoreactivities by ImageJ software (NIH, Bethesda, MD, USA) to estimate the fold increase at the rostral and caudal graft-host interfaces over baseline levels in uninjured parts of the cord (Iannotti et al., 2004; Tysseling-Mattiace et al., 2008).

Histological assessments of cavitation

Both rostral and caudal segments containing the guidance channel were stained for cresyl violet-eosin. Areas of lesion cavities were outlined and quantified using an Olympus BX60 microscope equipped with a Neurolucida system (MicroBrightField, Colchester, VT, USA) (Liu et al., 2006).

Quantification of axons and blood vessels within the guidance channel

Transverse slices of the grafts at their midpoint with the intact left hemicord were stained in 1% toluidine blue. The myelinated, unmyelinated axons as well as vessels inside the transplanted cables were counted using the Neurolucida software.

Characterization of axonal orientation

To determine the orientation of regenerated axons that just enter the graft, SMI-31-IR axons were randomly selected at the graft side of the interface, and a 'best fit' line was traced over each axon using ImageJ software. Because the filaments were aligned in a longitudinal direction parallel with the grafted guidance channels, we determined an axon angle by measuring the angle between a particular axon line and the longitudinal axis of the graft. An angle of 0° is considered parallel and 90° is considered perpendicular to the longitudinal axis of the regenerative tissue cable. Thirty randomly chosen axons in each section were analyzed and the mean and median angles were determined.

Statistical analysis

Data were expressed as mean ± standard deviation (SD). One-way analysis of variance with Tukey's *post hoc* test was used to determine statistical significance. A P value of < 0.05 was considered statistically significant. GraphPad Prism 3.0 (GraphPad Software, San Diego, CA, USA) was used.

Results

Low density filament entubulation induces greater axonal regeneration

In vitro, filament bundles with individual filament diameter of 5 μm provided better directionality and greater neurite growth potential of dorsal root ganglion neurons (Wen and Tresco, 2006). Compared with the non-filament group (**Figure 1A**), regenerated cables packed with filaments showed bigger cross sectional areas (**Figure 1B**–**D**). The denser the filaments were packed, the bigger the sizes of cables were found. The filaments took up a large proportion of the cross sectional space. Regenerated axons and blood vessels were distributed in the interspace among filaments (**Figure 1F**–**H**). Compared with the no filament control group, axonal regeneration and revascularization in all filament groups were significantly higher (P = 0.0037). However, increasing filament density did not enhance axonal regeneration and revascularization. The low density filament group had the greatest number of regenerated axons and blood vessels as compared to the medium density (P = 0.028) and high density groups (P = 0.033; **Figure 1I** and **J**).

Filament entubulation reduces lesion cavity, glial reaction and inflammation

Our data showed that at both the rostral and caudal graft-host interfaces, lesion cavity in all filament groups was reduced (P = 0.0002, *versus* no filament). There was no difference among different filament groups (**Figure 2A**–**E**). After injury, the expression of GFAP was increased at rostral and caudal edges of the host tissue. The extent and intensity of GFAP immunoreactivity (IR) in all filament groups were lower than that in the no filament group (**Figure 2F**–**J**) (P = 0.0044 or P = 0.00061, *versus* no filament). In the no filament group, numerous ED-1 positive macrophages were seen in clusters (**Figure 2K**). In contrast, grafts containing filaments

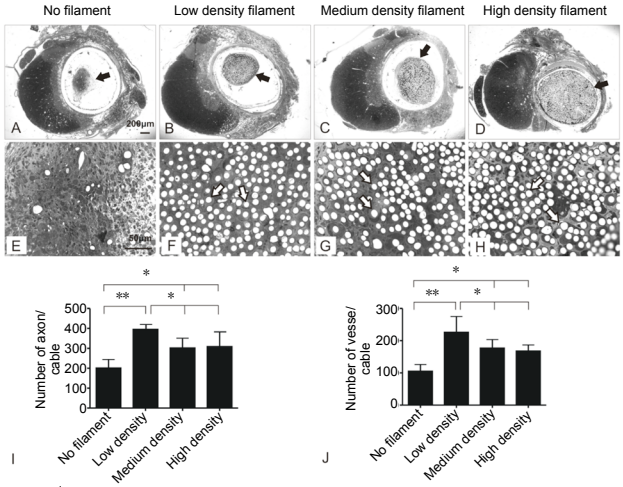

Figure 1 | Effect of filament density on axonal growth within the graft environment.

(A–D) Toluidine blue-stained semi-thin cross sections at the graft midpoint show guidance channels on the right and intact hemicord on the left. Regenerative tissue cables (black arrows in A–D) within the guidance channels were clearly seen in each of the four experimental groups. (E–H) Higher magnification of corresponding regenerative tissue cables in A–D shows clearly cross sectional filaments in F–H (arrows) but not E (no filament control). (I, J) Quantitative comparison of the mean number ± SD of myelinated axons (I) and blood vessels (J) among different groups. Poly (acrylonitrile-co-vinyl chloride) (PAN-PVC) hollow channels packed with 1000, 2000, and 4000 filaments were defined as low, middle and high density groups and were compared with empty channels as controls. *P < 0.05, **P < 0.01 (one-way analysis of variance with Tukey's *post hoc* test).

demonstrated a reduction of infiltrated macrophages (P = 0.0052 or P = 0.0007, *versus* no filament) that dispersedly distributed at the graft-host interface (**Figure 2L**–**O**).

Effect of different filament coating molecules on axonal regeneration

To determine the effects of different coating molecules on axonal regeneration *in vivo*, neurite outgrowth on filaments precoated with laminin, Matrigel or hydrogel was assessed. Myelinated axons in the middle of the graft were compared. Filaments treated with either laminin (**Figure 3D**, **H**, **L** and **M**) or Matrigel (**Figure 3C**, **G**, **K** and **M**) supported more axonal regeneration (P = 0.028 or P = 0.0084, *versus* no coated filament). Filaments treated with laminin and Hydrogel were preferable for new blood vessel growth (**Figure 3F**, **H** and **N**, P = 0.037 or P = 0.0054, *versus* no-coated filament). Laminin and Matrigel could also attract glial cell migration into the filament environment (**Figure 3I**–**L**), which might have played a role in promoting axonal regeneration.

Effect of laminin coating, combined with SCs and GDNF, on axonal regeneration

We then tested whether addition of SC and GDNF within the laminin-coated low density filament entubulation would promote further growth of axons and blood vessels as compared with either no filament or no SCs/GDNF (**Figure 4**). All three groups demonstrated a regenerative tissue cable in the graft mid-point including both myelinated and unmyelinated axons. However, combination of SCs, GDNF and laminin-coated filaments resulted in the greatest axonal regeneration (**Figure 4J**; laminin-coated filament + SCs/GDNF: 7469.5 ± 932.75; SCs/GDNF only: 2666.9 ± 248.5; laminin-coated filament only: 2215.75 ± 232.82; p =0.0006, *versus* SCs/GDNF only or laminin-coated filament only, quantification of regenerated axons from toluidine-blue stained semi-thin section). In EM image, we also found much more unmyelinated axons which cannot be clearly recognized in semi-thin sections due to low resolution toluidine-blue staining (**Figure 4E**, **F**, **H**, and **I**). Therefore, the number of total

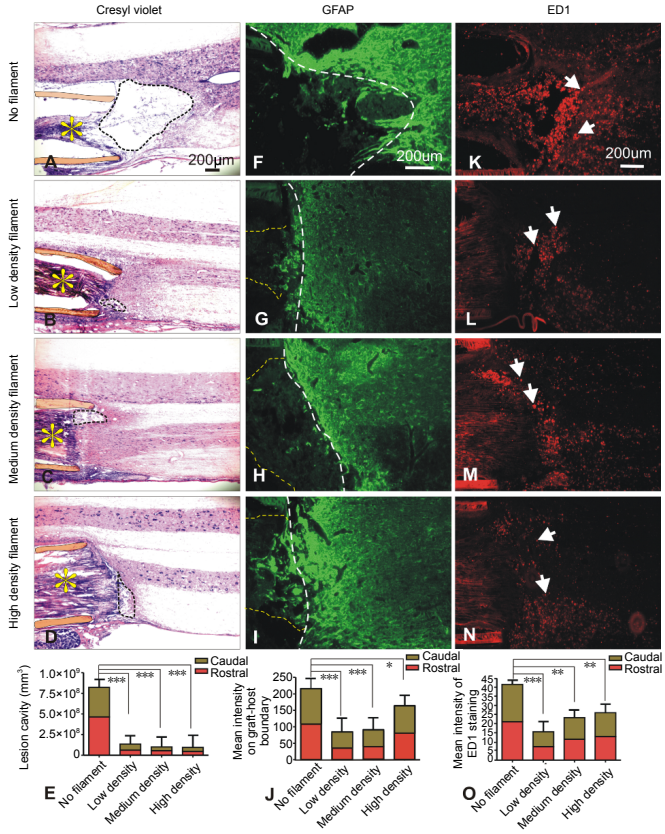

Figure 2 | Effect of filament density on lesion cavitation, astrocytic glial response, and macrophage infiltration.
(A–D) Crysel violet staining shows horizontal sections of spinal cords. The regenerative tissue cables (yellow asterisks) and the guidance channel walls (orange shaded) are clearly seen. At the caudal graft-host interface, marked cavity reduction was seen only in groups receiving filament entubulation (B–D, dashed circles) as compared to the non-filament entubulation (A, dashed circle). (E) Quantification of combined lesion cavity obtained from both rostral and caudal interfaces (***P < 0.001). (F–I) Glial fibrillary acidic protein (GFAP) immunostaining show strong GFAP-immunoreactivity (IR) in a case receiving no-filament entubulation (F); such GFAP immunoreactivity (GFAP-IR) was markedly reduced in groups receiving filament entubulation (G–I) particularly in the low (G) and medium (H) filament density groups. Yellow dashed lines indicate regenerative tissue cables and white dashed lines indicate the graft-host interfaces. (K–N) ED-1 immunostaining shows extent of activated macrophage infiltration (white arrows) at the caudal graft-host interfaces. Filament entubulation markedly reduced ED-1 immunoreactive (ED-1-IR) macrophage infiltration (L–N) as compared to no filament entubulation (K). (J, O) Quantification of relative optical intensity of GFAP-IR (*P < 0.05, ***P < 0.001; J) and ED-1-IR (**P < 0.01, ***P < 0.001; O). Poly (acrylonitrile-co-vinyl chloride) (PAN-PVC) hollow channels packed with 1000, 2000, and 4000 filaments were defined as low, middle and high density groups and were compared with empty channels as controls. (E, J, O) Data are expressed as the mean ± SD. One-way analysis of variance with Tukey's *post hoc* test was used. PAN-PVC hollow channels packed with 1000, 2000, 4000 filaments were defined as low, middle and high density groups and were compared with empty channels as controls.

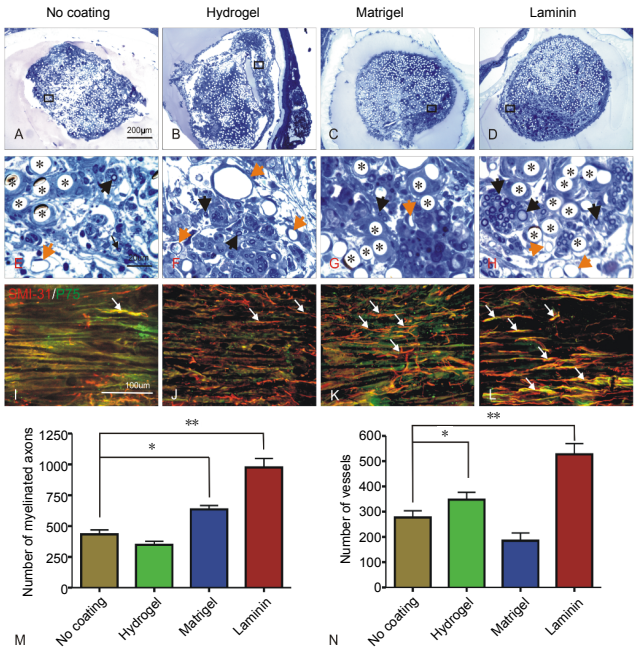

Figure 3 | Effect of different coating molecules on axonal regeneration.
(A–D) Toluidine blue-stained semi-thin cross sections at the graft midpoint show regenerative tissue cables containing filaments coated with different coating molecules. (E–H) High magnification of demarcated regions in A–D shows representative filaments (*), myelinated axons (black arrows) and blood vessels (brown arrows). (I–L) In all groups, regenerated axons (SMI-31-IR, red) were shown to be closely associated with endogenous Schwann cells (p75-IR, green) migrated from the host into the graft region (white arrows). (M, N) Quantitative comparison of the number of myelinated axons (M) and blood vessels (N) among different experimental groups (*P < 0.05, **P < 0.01). Data are expressed as the mean ± SD. One-way analysis of variance with Tukey's *post hoc* test was used. We examined the effects of different coating materials including laminin, Matrigel, and hydrogel by precoating them on low density channels since such density promoted the greatest axonal regeneration. No coating filaments served as control.

regenerated axons could be significantly underestimated. The distributive pattern of regenerated axons differs markedly among groups. In the SCs/GDNF only group, regenerated axons were dispersedly distributed (**Figure 4D** and **G**). On contrary, in both laminin-coated filament groups, with or without SCs/GDNF, myelinated and unmyelinated axons were seen to form fascicles (**Figure 4E**, **H**, **F**, and **I**). Finally, both laminin-coated filaments groups contained similar number of blood vessels which were significantly higher than the SC-GDNF only group but no statistically difference was found between the two laminin-filaments groups (laminin-coated filament + SCs/GDNF: 397.36 ± 97.65; laminin-coated filament only: 401.94 ± 112.6; *versus* SCs/GDNF only: 254.42 ± 48.1; P = 0.041) (**Figure 4K**).

Laminin-coated filaments guide directional growth of axons

In channels containing SCs and GDNF but no filaments, SMI-31 stained axons were randomly oriented (50.44 ± 15.43°) and were associated with p75-positive SCs (**Figure 5A**–**C**). In channels containing laminin-coated filaments, either with or without SCs/GDNF, fascicles of uniformly distributed axons were found and were strikingly aligned parallelly to the longitudinal axis of the filaments (**Figure 5D**–**I**). (laminin-coated filament + SCs/GDNF: 15.35 ± 11.80°; laminin-coated filament only, 14.46 ± 10.54°). Evidently, regenerated axons and SCs were well aligned and in close apposition along the grafted filaments (**Figure 5F** and **I**).

Discussion

Adult CNS neurons failed to regenerate axons after injury mainly due to the appearance of regeneration unfavorable extracellular milieu and shortage of physical and chemical cues eliciting and guiding axonal outgrowth (Hoffman-Kim et al., 2010; Lam et al., 2010; Qi et al., 2013). The utility of longitudinally oriented scaffolds such as magnetically aligned collagen gels and individual filaments, provided physical guidance and mimic the topography and orientation of axonal fascicles within the white matter for axon outgrowth (Xu et al., 1995; Rangappa et al., 2000). When combined with an appropriate adhesive coating, the filamentous structures become similar to the natural filamentous substrates present during CNS development. The current study represents the first attempt to characterize the contribution of filament density, coating molecules, SCs, and GDNF, in various combinations, to CNS axonal regeneration and directionality in

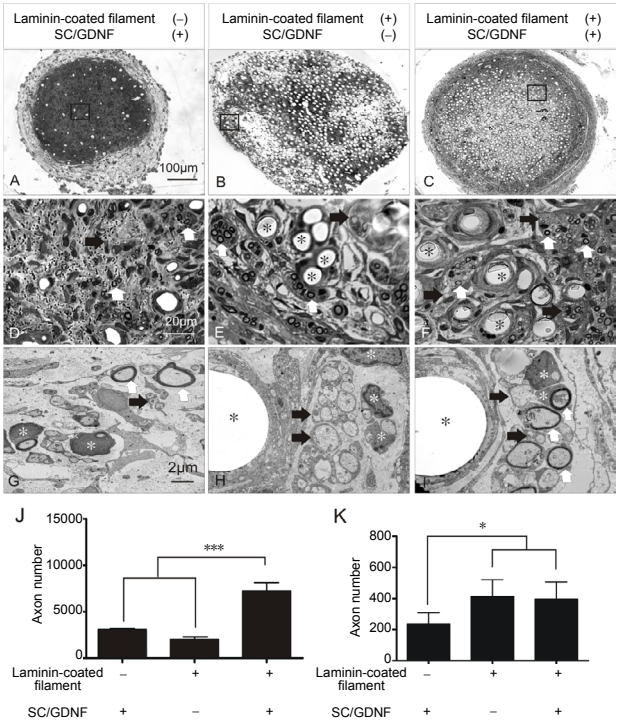

Figure 4 | Effect of laminin-coated filaments, combined with SCs and GDNF, on axonal regeneration.
(A–D) Toluidine blue-stained semi-thin cross sections at the graft midpoint show regenerative tissue cables containing SCs/GDNF without filaments (A), laminin-coated filaments (B) and combination of the two (C). (D–F) High magnification of demarcated regions (box area) in A–C shows representative filaments (E, F, *), myelinated axons (white arrows) and unmyelinated axons (black arrows). (G–I) Electron microscopic images of corresponding groups show that numerous myelinated (white arrows) and unmyelinated (black arrows) axons are present within the tissue cable. These fascicles of axons were closely associated with laminin-coated filaments (black asterisks) in the two filament entubulation groups (H, I). White asterisks indicate Schwann cells and myelin. (J, K) Quantitative comparison of the total number of regenerated axons and blood vessels among different experimental groups (*P < 0.05, ***P < 0.001). Data are expressed as the mean ± SD. One-way analysis of variance with Tukey's *post hoc* test was used. We tested the efficacy of the combination of laminin-precoated low density filaments, SCs, and GDNF. Channels containing SCs/GDNF but no filament or channels containing laminin precoated filament but no SCs/GDNF were served as controls. GDNF: Glial cell line-derived neurotrophic factor; SC: Schwann cell.

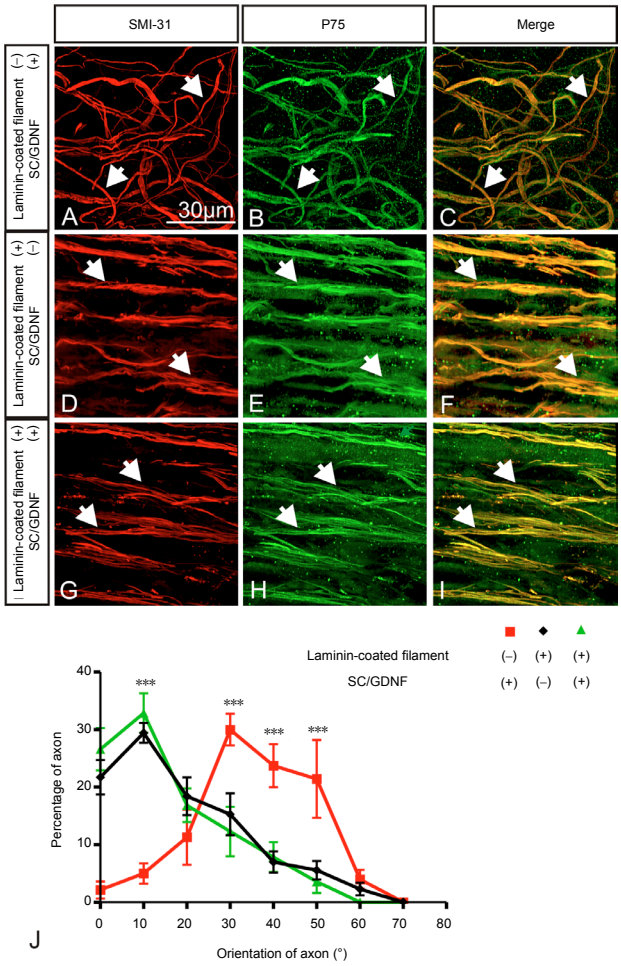

Figure 5 | Effect of laminin-coated filaments, combined with SCs and GDNF, on axonal orientation.
(A–I) Immunofluorescence staining shows regenerated axons (SMI-31-IR, arrows) and associated Schwann cells (p75-IR, arrows) in groups receiving SCs/GDNF without filaments (A–C), laminin-coated filaments (D–F) and combination of the two (G–I). In the group receiving SCs/GDNF without filaments, axons and associated SCs displayed a random orientation (A–C). On the contrary, in both laminin-coated filaments groups, fascicles of axons, along with associated SCs, grew unidirectionally and were in alignment with laminin-coated filaments (D–I) (white arrows indicate regenerated axons). (J) Quantitative comparison of axonal orientation among different groups (***P < 0.001). An angle of 0°is considered parallel and 90°is considered perpendicular to the longitudinal axis of the regenerative tissue cable. Data are expressed as the mean ± SD. One-way analysis of variance with Tukey's *post hoc* test was used. We tested the efficacy of the combination of laminin-precoated low density filaments, SCs, and GDNF. Channels containing SCs/GDNF but no filament or channels containing laminin precoated filament but no SCs/GDNF served as controls. GDNF: Glial cell line-derived neurotrophic factor; SC: Schwann cell.

a spinal cord hemisection and bridge transplantation model.

Effect of different filament densities on axonal regeneration

Axons from the CNS can grow along the filaments indicating the compatibility of filaments as guidance cues for axon regeneration. However, increasing filament density did not recruit more axonal growth into the graft, possibly because more filaments left less space for axonal growth which suggests that the appropriate substrate density optimize axonal regeneration. Our previous results indicated that Schwann cell migration along the filaments slightly preceded neurite outgrowth suggesting that SCs secreting adhesive molecules may provide a pathway for neurite extension (Wen and Tresco, 2006). Lack of these adhesive proteins may account for limited permissiveness of axonal growth along untreated filaments (Deumens et al., 2004; Hurtado et al., 2006).

Effect of filament entubulation on cavitation, astrogliosis and inflammation

After SCI, reactive astrocytes and cyst formation are major impediment for axonal regeneration (Meiners et al., 1995). Inflammatory cells result in increases in lesion size, neuronal death, and decreases in axonal growth or sparing as a result of primary and secondary responses to the injury (Awad et al., 2008; Liu et al., 2008). Although mechanisms of action remain to be investigated, we found that filament entubulation reduced lesion cavity, astrogliosis and inflammatory response at both rostral and caudal ends of the graft-host interfaces. The reduced lesion cavity may be related to the alleviation of glial and inflammatory responses and prevention of axonal die back or tissue retraction.

Effect of coated filaments, combined with SCs and GDNF, on axonal regeneration

Extracellular molecules (ECMs) cues have been reported to induce axon regeneration, cell migration and blood vessel growth (Dubovy et al., 2001; Costa et al., 2002; Blackmore and Letourneau, 2006). We found greater number of fasciculated axons within the laminin- and Matrigel-coated filament graft.

More host-derived SCs migrated into the ECM-coated filament grafts and myelinated regenerated axons. These regenerated axon-myelin units formed parallel fascicles running amongst bundles of filaments in a longitudinal orientation. At the EM level, numerous unmyelinated axons were found within these fascicles. Previously, we grafted SC and GDNF, into hemisected spinal cord and observed axonal regeneration and remyelination (Deng et al., 2011, 2013). When combined with laminin coated filaments, due to dual effects of the laminin and GDNF on migration, survival of host and grafted SCs, axonal regeneration and remyelination was significantly enhanced. In the group when SCs/GDNF were added to the laminin-coated filament entubulation, as high as 7,469 regenerated axons were found in the graft mid-point.

Effect of filaments on orientation of regenerated axons

Unidirectional axonal growth is necessary for efficient functional regeneration. Unorganized and randomly oriented axonal growth may lead to failure of reaching the target. The mechanical contact by unidirectional oriented texture of the growth surface could be transduced by the growth cone into axonal growth toward an appropriate target (Krayanek and Goldberg, 1981). Strong correlations have been documented between growth cone distribution, substrate topography, and the direction of neurite growth (Rajnicek et al., 1997; Rajnicek and McCaig, 1997). The energy of growth cone extension may be the underlying mechanism of the effect of filament on neurite directionality. When the filament size is in the cellular or subcellular size range, growth cones may easily sense the energy differences of different outgrowth directions. When combined with permissive cells (e.g. SCs), and trophic factors (e.g. GDNF), the orientational guiding effect of filament become prominent.

Conclusion

The present study showed that in the hemisected spinal cord, an entubulation configuration containing longitudinally aligned polypropylene filaments reduced tissue damage, astrogliosis and inflammatory response at the graft-host interface. Laminin coated filaments promoted unidirectional axonal regeneration. Combination of exogenous SCs and GDNF can synergistically enhance this regenerative effect resulting in a remarkable axonal growth into the graft environment. This combined strategy may provide a unique and optimal environment for long-distance functional axonal regeneration critical for the repair of human SCIs.

Acknowledgments: *We thank Patti L. Raley (Department of Neurological Surgery, Indiana University School of Medicine) for critical reading of the manuscript.*

Author contributions: *LXD and XMX designed experiments, performed experiments, collected and analyzed data and wrote the manuscript; RNW developed bioengineered materials; XW designed experiments, provided bioengineered materials, and approved the manuscript; NKL and SNY performed experiments, collected data, read and approved the manuscript. All authors approved the final version of the paper.*

Conflicts of interest: *The authors declare that they have no conflict of interest.*

Financial support: *Research in the Xu laboratory is supported by NIH 1R01 100531, 1R01 NS103481, Merit Review Award I01 BX002356, I01 BX003705, I01 RX002687 from the U.S. Department of Veterans Affairs, and Mari Hulman George Endowment Funds.*

Institutional review board statement: *This study was approved by Indiana University Institutional Animal Care and Use Committees (IACUC #:11011) on October 29, 2015.*

Copyright license agreement: *The Copyright License Agreement has been signed by all authors before publication.*

Data sharing statement: *Datasets analyzed during the current study are available from the corresponding author on reasonable request.*

Plagiarism check: *Checked twice by iThenticate.*

Peer review: *Externally peer reviewed.*

References

Awad H, Suntres Z, Heijmans J, Smeak D, Bergdall-Costell V, Christofi FL, Magro C, Oglesbee M (2008) Intracellular and extracellular expression of the major inducible 70kDa heat shock protein in experimental ischemia-reperfusion injury of the spinal cord. Exp Neurol 212:275-284.

Bamber NI, Li H, Lu X, Oudega M, Aebischer P, Xu XM (2001) Neurotrophins BDNF and NT-3 promote axonal re-entry into the distal host spinal cord through Schwann cell-seeded mini-channels. Eur J Neurosci 13:257-268.

Blackmore M, Letourneau PC (2006) L1, beta1 integrin, and cadherins mediate axonal regeneration in the embryonic spinal cord. J Neurobiol 66:1564-1583.

Costa S, Planchenault T, Charriere-Bertrand C, Mouchel Y, Fages C, Juliano S, Lefrancois T, Barlovatz-Meimon G, Tardy M (2002) Astroglial permissivity for neuritic outgrowth in neuron-astrocyte cocultures depends on regulation of laminin bioavailability. Glia 37:105-113.

Deng LX, Hu J, Liu N, Wang X, Smith GM, Wen X, Xu XM (2011) GDNF modifies reactive astrogliosis allowing robust axonal regeneration through Schwann cell-seeded guidance channels after spinal cord injury. Exp Neurol 229:238-250.

Deng LX, Deng P, Ruan Y, Xu ZC, Liu NK, Wen X, Smith GM, Xu XM (2013) A novel growth-promoting pathway formed by GDNF-overexpressing Schwann cells promotes propriospinal axonal regeneration, synapse formation, and partial recovery of function after spinal cord injury. J Neurosci 33:5655-5667.

Deumens R, Koopmans GC, Den Bakker CG, Maquet V, Blacher S, Honig WM, Jerome R, Pirard JP, Steinbusch HW, Joosten EA (2004) Alignment of glial cells stimulates directional neurite growth of CNS neurons in vitro. Neuroscience 125:591-604.

Dubovy P, Svizenska I, Klusakova I, Zitkova A, Houst'Ava L, Haninec P (2001) Laminin molecules in freeze-treated nerve segments are associated with migrating Schwann cells that display the corresponding alpha6beta1 integrin receptor. Glia 33:36-44.

Grimpe B, Dong S, Doller C, Temple K, Malouf AT, Silver J (2002) The critical role of basement membrane-independent laminin gamma 1 chain during axon regeneration in the CNS. J Neurosci 22:3144-3160.

Hoffman-Kim D, Mitchel JA, Bellamkonda RV (2010) Topography, cell response, and nerve regeneration. Annu Rev Biomed Eng 12:203-231.

Hurtado A, Moon LD, Maquet V, Blits B, Jerome R, Oudega M (2006) Poly (D,L-lactic acid) macroporous guidance scaffolds seeded with Schwann cells genetically modified to secrete a bi-functional neurotrophin implanted in the completely transected adult rat thoracic spinal cord. Biomaterials 27:430-442.

Iannotti C, Li H, Yan P, Lu X, Wirthlin L, Xu XM (2003) Glial cell line-derived neurotrophic factor-enriched bridging transplants promote propriospinal axonal regeneration and enhance myelination after spinal cord injury. Exp Neurol 183:379-393.

Iannotti C, Zhang YP, Shields CB, Han Y, Burke DA, Xu XM (2004) A neuroprotective role for glial cell line-derived neurotrophic factor following moderate spinal cord contusion injury. Exp Neurol 189:317-332.

Krayanek S, Goldberg S (1981) Oriented extracellular channels and axonal guidance in the embryonic chick retina. Dev Biol 84:41-50.

Lam HJ, Patel S, Wang A, Chu J, Li S (2010) In vitro regulation of neural differentiation and axon growth by growth factors and bioactive nanofibers. Tissue Eng Part A 16:2641-2648.

Liu N, Han S, Lu PH, Xu XM (2004) Upregulation of annexins I, II, and V after traumatic spinal cord injury in adult rats. J Neurosci Res 77:391-401.

Liu NK, Zhang YP, Titsworth WL, Jiang X, Han S, Lu PH, Shields CB, Xu XM (2006) A novel role of phospholipase A2 in mediating spinal cord secondary injury. Ann Neurol 59:606-619.

Liu NK, Zhang YP, Han S, Pei J, Xu LY, Lu PH, Shields CB, Xu XM (2007) Annexin A1 reduces inflammatory reaction and tissue damage through inhibition of phospholipase A2 activation in adult rats following spinal cord injury. J Neuropathol Exp Neurol 66:932-943.

Liu WL, Lee YH, Tsai SY, Hsu CY, Sun YY, Yang LY, Tsai SH, Yang WC (2008) Methylprednisolone inhibits the expression of glial fibrillary acidic protein and chondroitin sulfate proteoglycans in reactivated astrocytes. Glia 56:1390-1400.

McKeon RJ, Hoke A, Silver J (1995) Injury-induced proteoglycans inhibit the potential for laminin-mediated axon growth on astrocytic scars. Exp Neurol 136:32-43.

Meiners S, Powell EM, Geller HM (1995) A distinct subset of tenascin/CS-6-PG-rich astrocytes restricts neuronal growth in vitro. J Neurosci 15:8096-8108.

Qi L, Li N, Huang R, Song Q, Wang L, Zhang Q, Su R, Kong T, Tang M, Cheng G (2013) The effects of topographical patterns and sizes on neural stem cell behavior. PLoS One 8:e59022.

Rajnicek A, McCaig C (1997) Guidance of CNS growth cones by substratum grooves and ridges: effects of inhibitors of the cytoskeleton, calcium channels and signal transduction pathways. J Cell Sci 110 (Pt 23):2915-2924.

Rajnicek A, Britland S, McCaig C (1997) Contact guidance of CNS neurites on grooved quartz: influence of groove dimensions, neuronal age and cell type. J Cell Sci 110 (Pt 23):2905-2913.

Rangappa N, Romero A, Nelson KD, Eberhart RC, Smith GM (2000) Laminin-coated poly(L-lactide) filaments induce robust neurite growth while providing directional orientation. J Biomed Mater Res 51:625-634.

Sorensen A, Alekseeva T, Katechia K, Robertson M, Riehle MO, Barnett SC (2007) Long-term neurite orientation on astrocyte monolayers aligned by microtopography. Biomaterials 28:5498-5508.

Talac R, Friedman JA, Moore MJ, Lu L, Jabbari E, Windebank AJ, Currier BL, Yaszemski MJ (2004) Animal models of spinal cord injury for evaluation of tissue engineering treatment strategies. Biomaterials 25:1505-1510.

Titsworth WL, Liu NK, Xu XM (2008) Role of secretory phospholipase a(2) in CNS inflammation: implications in traumatic spinal cord injury. CNS Neurol Disord Drug Targets 7:254-269.

Titsworth WL, Onifer SM, Liu NK, Xu XM (2007) Focal phospholipases A2 group III injections induce cervical white matter injury and functional deficits with delayed recovery concomitant with Schwann cell remyelination. Exp Neurol 207:150-162.

Tysseling-Mattiace VM, Sahni V, Niece KL, Birch D, Czeisler C, Fehlings MG, Stupp SI, Kessler JA (2008) Self-assembling nanofibers inhibit glial scar formation and promote axon elongation after spinal cord injury. J Neurosci 28:3814-3823.

Wen X, Tresco PA (2006) Effect of filament diameter and extracellular matrix molecule precoating on neurite outgrowth and Schwann cell behavior on multifilament entubulation bridging device in vitro. J Biomed Mater Res A 76:626-637.

Xu XM, Guenard V, Kleitman N, Bunge MB (1995) Axonal regeneration into Schwann cell-seeded guidance channels grafted into transected adult rat spinal cord. J Comp Neurol 351:145-160.

Xu XM, Zhang SX, Li H, Aebischer P, Bunge MB (1999) Regrowth of axons into the distal spinal cord through a Schwann-cell-seeded mini-channel implanted into hemisected adult rat spinal cord. Eur J Neurosci 11:1723-1740.

Zhang N, Zhang C, Wen X (2005) Fabrication of semipermeable hollow fiber membranes with highly aligned texture for nerve guidance. J Biomed Mater Res A 75:941-949.

C-Editors: Zhao M, Li CH; T-Editor: Jia Y